Lipid Order–Disorder Transitions in Complexes of Melittin and Ditetra- and Dipentadecanoylglycerophosphocholines†

F. G. Prendergast,* J. Lu, G. J. Wei, and V. A. Bloomfield

ABSTRACT: The interaction of melittin (MLT), a 26 amino acid peptide isolated from bee venom, with diacylglycerophosphocholine has been examined by application of light scattering and fluorescence techniques. Melittin interacts most strongly with ditetradecanoylglycerophosphocholine (DMPC) and dipentadecanoylglycerophosphocholine (DPenPC) at their phase transition temperatures (T_c). Light scattering shows that the interaction with DMPC at melittin:lipid ratios of 1:400 or greater is multiphasic with respect to time. At 25 °C, there is first an increase in turbidity, then an apparently cooperative decrease in light scattering, and finally a clearing of the solution. The apparent rates of all stages of the interaction increase markedly with increase in MLT:lipid ratio. The fluorescence anisotropy (r_{ss}) of diphenylhexatriene (DPH) embedded in the lipid bilayers shows a biphasic increase to an apparent equilibrium value. Attainment of the latter coincides with a minimum intensity plateau in the light scattering signal. Quasi-elastic light scattering (QLS) and electron microscopy data show that at MLT:lipid ratios of 1:400 to 1:100, homogeneous mixed (protein–lipid) micelles are formed with dimensions of 210–250 Å. The micelles apparently do not have a trapped volume and are assumed to be nonvesicular structures. Measurements of r_{ss} and differential phase fluorometry were used to show that the structure formed at equilibrium exhibits an order parameter for DPH that is in excess of that observed for DPH in the gel phase of DMPC or DPenPC vesicles only. The MLT–DMPC or MLT–DPenPC complexes monitored by changes in r_{ss} for DPH exhibit a highly cooperative thermal transition at 31 and 41 °C (compared with 24 and 33 °C for DMPC and DPenPC vesicles, respectively) when melittin:lipid ratios are ca. 1:400 to 1:100. However, at higher ratios of peptide:lipid the transition becomes increasingly broadened, and at a 1:1 peptide:lipid ratio there is no detectable phase transition. The pattern of DPH fluorescence anisotropy changes is mirrored by that of a cationic analogue, trimethylammonium diphenylhexatriene (TMA-DPH), which was used to minimize the probability of adsorption of the fluorophore near the cationic peptide. QLS indicates a marked increase in the size of the MLT–lipid mixed micelles from ca. 220 to 1220 Å and delineates an apparent phase transition. Measurements of r_{ss} of DPH made on thermally equilibrated samples show no difference in profile whether the temperature is increased or decreased. However, QLS data on micellar size as the temperature is scanned showed marked hysteresis, and the micelles do not return to their original sizes. We deduce that with the saturated phospholipids, DMPC and DPenPC, MLT at low MLT:lipid ratios forms mixed micelles that (i) are of defined size, (ii) are highly ordered, and (iii) exhibit highly cooperative phase transitions at temperatures considerably higher than those of pure lipid. The last two properties are unprecedented among peptide–lipid complexes. The phase behavior may, however, depend on peptide:lipid ratios and the thermal history of the system.

The ability of melittin (MLT), a 26 amino acid peptide isolated from bee venom, to lyse cell membranes is well recognized (Habermann, 1965; Sessa et al., 1969), but the detailed molecular mechanisms that underlie its cytolytic action are as yet unclear.

Melittin is known to have a marked affinity for lipid. It interacts avidly with zwitterionic lipids (Habermann, 1965; Sessa et al., 1969; Mollay & Kreil, 1973; Dufourcq & Faucon, 1977; Lavialle et al., 1980), negatively charged phospholipids (Dufourcq & Faucon, 1977), and negatively or positively charged surfactants (Dawson et al., 1978; Knöppel et al., 1979) and apparently forms mixed micelles with nonionic detergents such as Brij 58 (Knöppel et al., 1979), Tween, or Triton-X (F. G. Prendergast, unpublished data). Not only is melittin cytolytic but also it effectively lyses artificial vesicles (Sessa et al., 1969) and causes marked conductance changes in black lipid membranes (Tosteson & Tosteson, 1981). Its ability to interact with lipids or micelles irrespective of the charge on the lipid implies that the main driving force for interaction is not electrostatic. Available evidence points toward a major role for hydrophobic interactions in the formation of melittin–lipid complexes (Dufourcq & Faucon, 1977; Brown et al., 1980; Lauterwein et al., 1979, 1980).

In many ways melittin appears to interact in a manner akin to that of apolipoproteins. The argument has been made, for example, that melittin can form an amphipathic helix (DeGrado et al., 1981) similar to those presumably formed by apolipoproteins (Wlodawer et al., 1979; Morrisett et al., 1977) or by synthetic peptide modeled after the apolipoproteins (Kanellis et al., 1980; Fukushima et al., 1979; Mao et al., 1981). On the strength of this argument, a synthetic analogue of melittin has been synthesized (DeGrado et al., 1981) and has been shown to be lytic with effects similar to those of melittin. From what is known about lipoprotein insertion into lipid, we might anticipate that melittin (i) would interact most rapidly at the phase transition temperature of vesicles (24 °C) and (ii) should cause an increase in the apparent order of the lipid but would lead to a broadened phase transition of the lipid.

Raman spectroscopic studies performed on MLT–DMPC complexes (Lavialle et al., 1980; Levin et al., 1982) at a melittin:lipid ratio of 1:14 revealed two order–disorder transitions. One occurred at 17 °C, which was 5.5 °C less than the thermal transition temperature (22.5 °C) observed for the

† From the Department of Pharmacology, Mayo Foundation, Rochester, Minnesota 55905 (F.G.P. and J.L.), and the Department of Biochemistry, College of Biological Sciences, University of Minnesota, Minneapolis, Minnesota 55108 (G.J.W. and V.A.B.). *Received June 14, 1982.* This work was supported in part by grants from the American Heart Association, Minnesota Affiliate, and National Institutes of Health Grant NIGMS-31241 and was done during tenure of an Established Investigatorship of the American Heart Association. F.G.P. is a Searle Foundation Scholar. The QLS work was supported by National Science Foundation Grant PCM 7806777 to V.A.B.

0006-2960/82/0421-6963$01.25/0

DMPC preparation. This appeared to reflect a peptide-induced depression of the main lipid phase transition. A second transition at 29 °C was ascribed to the "melting" of approximately seven immobilized "boundary lipid" molecules. At higher melittin:lipid ratios the apparent number of boundary lipids attached to melittin decreased. Electron spin resonance (ESR) techniques were used by Williams & Bell (1972) to show that melittin disrupted the phospholipid matrix of unilamellar vesicles prepared from egg lecithin, phosphatidylserine, and lipids extracted from *Escherichia coli*. However, they did not provide a detailed analysis of these interactions. ESR was also used by Hegner et al. (1973) to investigate the effect of melittin on red cells, their ghosts, and "spherules" formed from total erythrocyte lipids. They concluded that at low concentrations melittin caused an increase in "fluidity" of the apolar fatty acid chains but a decrease in fluidity at higher concentrations. From a nuclear magnetic resonance (NMR) study of MLT interaction with lysophosphatidylcholine micelles, Debony et al. (1979) found that melittin maximally perturbed (an upfield shift was noted) the methylene groups α and β to the ester bond. They concluded that this result was a consequence of ring current effects of the tryptophan moiety at position 19 of melittin on the lipid; but they did not pursue further the effect of melittin on the lipid dynamics.

Clearly, little is known about the state of the lipid in MLT–lipid complexes. The system is, however, superficially easy to work with and amenable to use of several biophysical techniques. We have used fluorescence and quasi-elastic light scattering techniques to ask three questions initially: (1) What are the kinetics of MLT interaction with phospholipids? (2) Do unique mixed micelles form (akin to those formed by apolipoproteins and DMPC)? (3) What is the thermotropic behavior of the MLT–lipid complexes? Our results indicate that (1) the kinetics of interaction are complex, (2) mixed MLT–lipid micelles of defined sizes can be formed, and (3) the micelles exhibit sharp cooperative phase transitions at temperatures well removed from those of the original lipid vesicles.

Experimental Procedures

Materials

Ditetradecanoylglycerophosphocholine (DMPC), dipentadecanoylglycerophosphocholine (DPenPC), and dioleoylglycerophosphocholine (DOPC) were purchased from Supelco, Bellefonte, PA, and were used without further purification. Dielaidoylglycerophosphocholine (DEPC) was purchased from P-L Biochemicals. Diphenylhexatriene (DPH) was purchased from Aldrich Chemical Co., and trimethylammonium diphenylhexatriene (TMA-DPH) was obtained as the *p*-toluenesulfonate salt from Molecular Probes, Plano, TX. All solvents used were HPLC grade purchased from Burdick and Jackson, Muskegon, MI.

Preparation of Melittin. Melittin was either obtained as a gift from Dr. J. Yunginger, Department of Immunology, Mayo Foundation, or purchased from Sigma Chemical Co., St. Louis, MO. Both preparations contained substantial phospholipase A_2 (PlA_2) activity and also a few other peptides (in low amounts) that were readily detectable by high-performance liquid chromatography (HPLC). Pure melittin was prepared by two procedures. In the first, impure melittin was subjected to preparative HPLC on a Waters C_{18} reverse-phase column, the eluent being a gradient of 0–50% acetonitrile in 2 mM phosphoric acid. The melittin peak separated clearly from the other peptides and PlA_2 and was collected and lyophilized after neutralization of the acid with sodium hydroxide. (The tryptophan residue of melittin appears to be especially photosensitive when placed in an acid medium; thus, rapid neutralization of the phosphoric acid was essential.) A sample of melittin so purified showed a single peak when rerun on the HPLC column. In the second, a solution of melittin in *water* was ultrafiltered through an Amicon YM-10 membrane. This membrane retained all of the PlA_2 activity, some of the melittin (possibly because of formation of melittin aggregates), and apparently most of a "brown" substance that contaminates melittin preparations. The melittin in the filtrate was then concentrated by ultrafiltration through an Amicon UM-05 membrane (molecular weight cutoff ~500). The melittin had to be "washed" at least twice by repeated filling of the ultrafiltration cell to eliminate a low molecular weight contaminant that showed a peak absorbance at 260 nm but also had substantial absorbance at 280 nm. The retentate from the UM-05 ultrafiltration was then lyophilized and the purity of the lyophilized peptide determined by HPLC as described above. Melittin prepared in this manner was >98% pure by HPLC analysis. Both preparations of melittin were also assayed for residual PlA_2 activity by (i) a fluorometric assay for this enzyme that employs dipyrenoylbutyroylglycerophosphocholine as a substrate (Hendrickson & Rauk, 1981) and can detect 10 ng of enzyme and (ii) crossed immunoelectrophoresis (Dr. J. Yunginger, personal communication of work done by Dr. H. Løwenstein, The Protein Laboratory, Copenhagen, Denmark). Neither method showed any PlA_2 activity in the "pure" melittin preparations. This emphasis on establishing the absence of PlA_2 in our melittin preparations is especially important because of the length of some of our experiments and because melittin is known to markedly enhance PlA_2 activity (Yunes et al., 1977). As we shall show shortly, the reversibility of some of the processes studied provides further and essential evidence for the absence of PlA_2 contamination in our preparations of pure melittin.

Methods

Preparation of Bilayer Vesicles. An aliquot of lipid dissolved in chloroform was placed in a crucible, fluorescent probe (DPH dissolved in $CHCl_3$ or TMA-DPH in CH_3CN) was added when needed to give a fluorophore:lipid ratio of 1:500, and the solvents were evaporated off under a stream of N_2 or argon. To the crucible was then added 10 mL of a solution containing 0.125 M KCl and 0.010 M 4-morpholinepropanesulfonic acid (Mops) at pH 7.0, and the mixture was sonicated for 10 min in 2-min bursts through the use of a Braunsonic sonifier set at 70 W. After sonication the vesicle suspension was annealed at a temperature at least 10 °C above the T_c for the lipid (or at 25 °C for vesicles of DOPC) for 0.5 h, and the preparations were then centrifuged at 16300*g* at 20 °C for 1 h. The supernatants were used for the experiments. Phospholipids were determined by the method of Ellefson & Caraway (1976).

Electron Microscopy. Samples of DMPC vesicles and DMPC–melittin complexes (lipid:MLT ratio 200:1) were prepared as described above, and bacitracin was added at 50 μg/mL to each sample as a wetting agent to promote even spreading. A formvar carbon coated grid (200 mesh, copper) was submerged in a small amount of sample, placed in a dish, covered, and incubated at room temperature for 20 min to allow the vesicles to stick to the grid. Excess liquid on the grid was then removed with filter paper and the grid immediately submerged in a small amount of 1% phosphotungsate, pH 5.5, for 30 s. The grid was then placed on filter paper and allowed to dry at room temperature. These "negatively stained" grids

were examined with a Phillips 400 electron microscope at a magnification of ×70 000.

Fluorescence and Light Scattering Measurements. Fluorescence intensities and spectra were measured in an SLM series 8000 photon counting spectrofluorometer. The fluorescence of DPH and TMA-DPH was excited at 360 nm with light passed through a monochromator (slits 4–8 nm) and a Corning 7-54 filter. Light scattering was measured at 90° in the same instrument. For these measurements 360-nm excitation light was used and the Rayleigh scattering monitored by placing a 5-nm band-pass interference filter (centered on 360 nm) in the emission path. Light-intensity measurements (whether light scattering or fluorescence) were always made as ratios of the intensity of the signal of interest to that of a reference quantum counter to cancel possible fluctuations due to variable output from the lamp source. This was especially critical for measurements made over long intervals of time.

Measurements of fluorescence lifetimes (τ), steady-state anisotropies, and differential phase fluorometry ($\Delta\tau$) were performed on an SLM subnanosecond fluorometer. Fluorescence lifetimes were measured by the phase-modulation method of Spencer & Weber (1969) with a polarizer oriented to 54.7° in the emission path to negate effects of Brownian motion on τ (Spencer & Weber, 1970). Measurements of $\Delta\tau$ were made as described by Mantulin & Weber (1977), Lakowicz & Prendergast (1978), and Lakowicz et al. (1979). An excitation wavelength of 360 nm (slits 0.5 mm) was used to excite the fluorescence of DPH and TMA-DPH (Prendergast et al., 1981). Fluorescence emission was isolated from Rayleigh and Raman scattering by placement of a Schott KV 418-nm filter in the emission path. Steady-state anisotropies were measured by operation of the instrument in a "T" format in the manner described by Weber & Bablouzian (1966). Again KV 418-nm filters were placed in the emission path to isolate fluorescence emission.

Calculations on Fluorescence Data. Steady-state anisotropies (r_{ss}) were calculated from the definition

$$r_{ss} = \frac{I_{\parallel} - I_{\perp}}{I_{\parallel} + 2I_{\perp}} \tag{1}$$

where $I_{\parallel}$ and $I_{\perp}$ represent the intensities of fluorescence emission polarized vertically and horizontally, respectively, when the excitation is vertically polarized. Limiting hindered anisotropies as measured by differential phase fluorometry ($r_{\infty},\Delta\tau$) were calculated from the relation

$$\tan\Delta = \frac{\omega\tau(r_0 - r_{\infty})(2R\tau)}{(1/9)m_0(1 + \omega^2\tau^2) + (1/3)S(2R\tau) + m_{\infty}(2R\tau)^2} \tag{2}$$

where

$$m_{\infty} = (1 + 2r_{\infty})(1 - r_{\infty})$$

and

$$S = 2 + r_0 - r_{\infty}(4r_0 - 1)$$

(Lakowicz et al., 1979). As we have pointed out elsewhere (Engel & Prendergast, 1981), $r_{\infty},\Delta\tau$ and r_{∞},t (the latter determined by time-resolved measurements) are the same under the conditions of the experiments described here but are not necessarily synonymous. The fluorescence order parameter, S, was then determined from the relation

$$r_{\infty}/r_0 = S^2 \tag{3}$$

(according to Jähnig, 1979a,b; Heyn, 1979; Lipari & Szabo, 1980; Engel & Prendergast, 1981). This relation holds providing that the substrate in which the probe is embedded does not contribute significantly to the depolarization of the fluorescence, i.e., does not exhibit a rotational correlation time similar to the fluorescence lifetime of the probe. If the substrate does rotate on the fluorescence lifetime scale of the probe, then the anisotropy data and, hence, S need to be corrected for the effect of substrate rotation (Prendergast, 1981; Engel & Prendergast, 1981; L. W. Engel and F. G. Prendergast, unpublished results).

Quasi-Elastic Light Scattering. Quasi-elastic and total intensity light scattering were measured by using an argon ion laser (operating at a wavelength of 488 nm), an ITT FW 130 photon-counting photomultiplier, and a Langley-Ford correlator. The apparatus and the method of data analysis have been described in detail elsewhere (Pletcher et al., 1980; Bloomfield & Lim, 1978). A cumulant fitting procedure (Koppel, 1972) was used to obtain z-averaged diffusion coefficients, which were then converted to hydrodynamic radii by the Stokes–Einstein equation. The "quality factor", defined as the ratio of the second cumulant to the square of the first cumulant, was used as an indication of the degree of polydispersity of the sample. At low melittin to lipid ratio (<0.01), the molecular weights of the lipid vesicles and the complex micelles were assumed to be proportional to the intensities of the scattered light, with the same proportionality constant. That is, scattering form factor correlations and minor differences in the refractive index increment between mellitin and lipid were ignored.

Results

Kinetics of Formation of Melittin–Lipid Complexes. The rates of insertion of peptides and proteins are known to be maximal at the phase transition temperature of the lipid, e.g., for apolipoprotein A-I interacting with DMPC (Pownall et al., 1978). Although maximum *rates* of melittin–DMPC interaction occur at T_c for the lipid, 23.9 °C, (F. G. Prendergast, unpublished data), the changes in light scattering and fluorescence are qualitatively the same at 25 °C, and the MLT–lipid complexes formed at 23.9 and 25 °C are identical for any given peptide:lipid ratio. (The latter temperature had been chosen for incubations during experiments designed to determine equilibrium binding constants for the MLT–lipid interactions.) At the outset, we determined that addition of melittin to DMPC vesicles caused irreversible lysis of the latter. This was shown by inclusion of either carboxyfluorescein diacetate (the fluorescence of which is concentration quenched in the vesicle) or [^{14}C]inulin in the internal volume of the vesicles. In the former instance, addition of melittin at 25 °C resulted in a rapid release of the fluorophore, which upon dilution in the bulk medium yielded intense fluorescence. The release of [^{14}C]inulin from vesicles by melittin action was shown by gel filtration (F. G. Prendergast, unpublished data).

The effects of melittin on DMPC vesicles are readily demonstrated by 90° light scattering measurements in a conventional fluorometer. At low peptide:lipid ratios the protein merely promotes an increase in light scattering, at least on the time scale of the experiment reported here (Figure 1A), but at higher ratios, the initial increase in light scattering is followed by a relatively rapid decrease in the intensity of the scattered light (Figure 1B). The response overall is clearly multiphasic. Figure 1B shows that the slopes of the rapid phases do not change significantly with higher melittin concentrations and that the apparent enhancement of reaction rates results from a shortening of the lifetime of the phase that shows increased light scattering. This conclusion is borne out by data not shown here for melittin:lipid ratios of 1:700, which clarified only after 48 h. The pattern of the rapid decrease

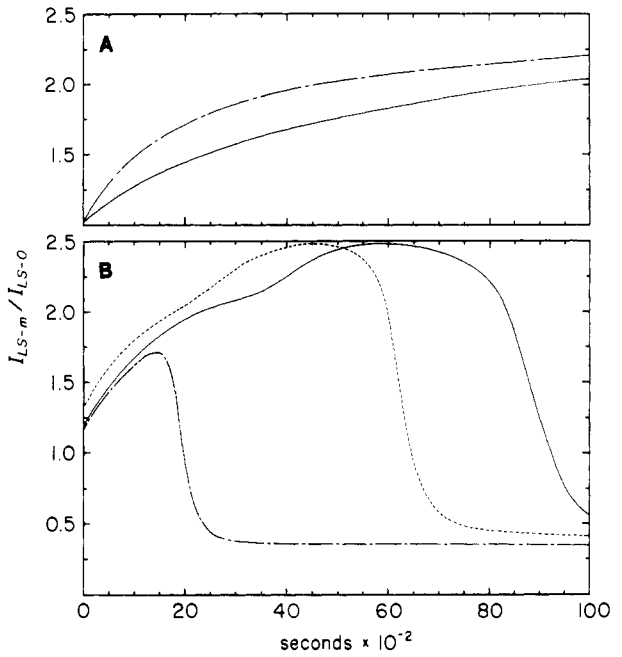

FIGURE 1: Changes in intensity of scattered light at 90° (expressed as ratio of measured intensity I_{LS-m} divided by initial intensity I_{LS-0}) of DMPC vesicles induced by addition of melittin. (A) At low peptide:lipid ratios [(—) and (- - -), MLT:DMPC ratios of 1:1000 and 1:600, respectively] melittin causes only an increase in light scattering over the time of the experiment. (B) At higher peptide:lipid ratios [(—), (---), and (- - -), MLT:lipid ratios of 1:400, 1:220, and 1:100, respectively] the profiles of I_{LS} changes are biphasic. Melittin was added at zero time.

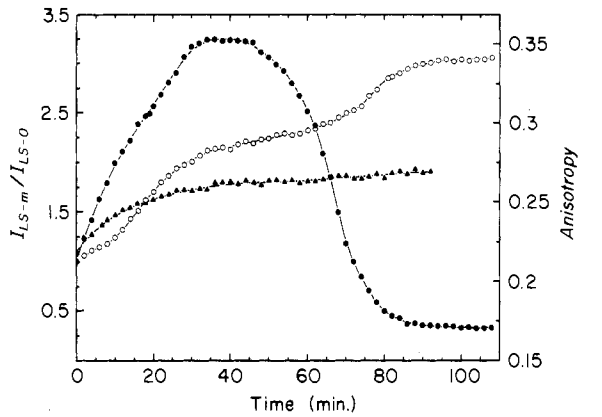

FIGURE 2: Comparative patterns of changes in light scattering (I_{LS}) of DMPC vesicles and fluorescence steady-state anisotropy for DPH embedded in DMPC vesicles caused by addition of melittin. Changes in 90° light scattering intensity of DMPC vesicles (I_{LS}) when melittin is added at 25 and 34 °C are given by the solid circles and solid triangles, respectively. The light scattering intensity of the melittin–lipid complex after 2 h was unchanging with time. The changes in anisotropy of DPH (open circles) occurred only when melittin was interacted with DMPC at or around the phase transition temperature of the lipid—in this instance the reaction was observed at 25 °C. For all experiments the MLT:lipid ratio was 1:200, and melittin was added at zero time.

strongly suggests a cooperative response. The data in Figure 2 show that at temperatures substantially above T_c of DMPC, addition of melittin leads merely to a slow increase in light scattering, at least at this lipid:peptide ratio and on the time scale reported there. Similar results were obtained with DPenPC and DEPC when studies were performed at their respective transition temperatures. At temperatures well below T_c we did not observe any melittin-induced changes in the intensity of scattered light; neither were any changes seen upon addition of melittin to vesicles of DOPC at peptide:lipid ratios

Table I: Representative Dimensions of DMPC Vesicles and Melittin–Lipid Mixed Micelles Determined by Quasi-Elastic Light Scattering and Electron Microscopy[a]

method	no.	sample (MLT:DMPC)	$2R_h$[b] (Å)	D[b] (10^{-7} cm²/s)	QF[b]	I[b] ($\times 10^{-4}$ cps)
QLS	1	DMPC (solo)	750	0.57	0.55	3.65
	2	1:80	238	1.80	0.10	10.30
	3	1:40	313	1.37	0.13	16.20
	4	1:20	700	0.61	0.27	3.84
	5	1:13	1250	0.34	0.45	3.00
	6[c]	1:10				
	7[c]	1:6.6				
					SD (Å)	
electron microscopy[d]	1	DMPC (solo)	850		±130	
	2	1:160	235		±15	
	3	1:80	225		±15	
	4	1:20[e]	1000		±200	
	5	1:60[f]	900		±200	

[a] All electron microscopy was done at room temperature. [b] $2R_h$ represents the diameter; D is the diffusion coefficient; QF refers to the quality factor (see text); I is the total light intensity in counts per second (cps). For the electron microscopy data, SD is the standard deviation. [c] These two samples (and to some extent no. 5) looked like a dispersion of oil in water; the light beam was dispersed, and there was large intensity fluctuation. [d] In order to calculate the dimensions, it was necessary to measure a minimum of 100 negatively stained images on electron micrographs. [e] The micrographs of MLT–DMPC mixed micelles at high peptide:lipid ratios showed multiple rouleaux. The discoid forms in the rouleaux had dimensions similar to the solitary forms on the micrographs. [f] This sample was first heated to 45 °C and then cooled to room temperature prior to processing for electron microscopy. The micrograph showed multiple rouleaux with discoid forms of dimensions like those given here.

of up to 1:75 (J. Lu and F. G. Prendergast, unpublished data).

Fluorescence experiments were then done on the same preparation of vesicles that was used for experiments described by the data in Figure 1. In Figure 2 the changes in r_{ss} for DPH embedded in DMPC vesicles at 25 °C upon addition of melittin are shown. The biphasic anisotropy profile is apparent and obviously related in time to the changes observed in the light scattering experiments. The maximum anisotropy value coincides precisely in time with the minimum light scattering signal, and both measurements show stable values for at least several days thereafter. It is important to note that the decrease in light scattering was not attended by precipitation of any material from solution; the clarified solution was always homogeneously fluorescent.

Characterization of Structure and Dynamics of Melittin–Lipid Complex. Quasi-elastic light scattering (QLS) data showed that the size of the equilibrium particle formed after interaction depended markedly on the peptide:lipid ratio. At both very low and very high ratios the complexes were larger than the original vesicles and clearly very heterogeneous, judging from the quality factors. At peptide:lipid ratios in the range 1:400 to 1:100, however, the melittin–DMPC (MLT–DMPC) complexes achieve a diameter, 250–200 Å, much smaller than that of the original vesicles (ca. 700 Å) and apparently more homogeneous in distribution (quality factors of 0.55 and 0.10 for the lipid vesicles and the MLT–DMPC complexes, respectively). Electron microscopic data corroborate those obtained by quasi-elastic light scattering (Table I) with regard to both size and degree of heterogeneity of the original vesicles and the melittin–lipid complexes. The electron micrographs also revealed that at peptide:lipid ratios <1:500, irregular peptide–lipid complexes were formed that were generally larger than the DMPC vesicles. Similar amorphous

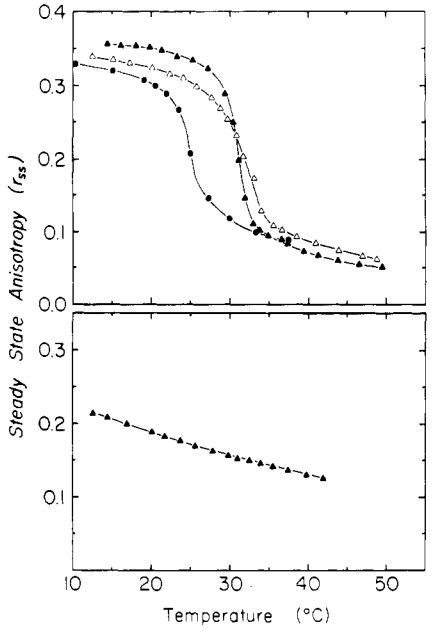

FIGURE 3: Effects of different melittin:lipid ratios on the steady-state anisotropy (r_{ss}) profiles of DPH embedded in DMPC as temperature is varied: (upper panel) r_{ss} values for DMPC vesicles only (●) and r_{ss}–temperature profiles of the melittin–lipid complex at peptide:lipid ratios of 1:100 (▲) and 1:30 (△); (lower panel) r_{ss} of DPH in melittin–lipid mixed micelle of 1:1 peptide:lipid ratio.

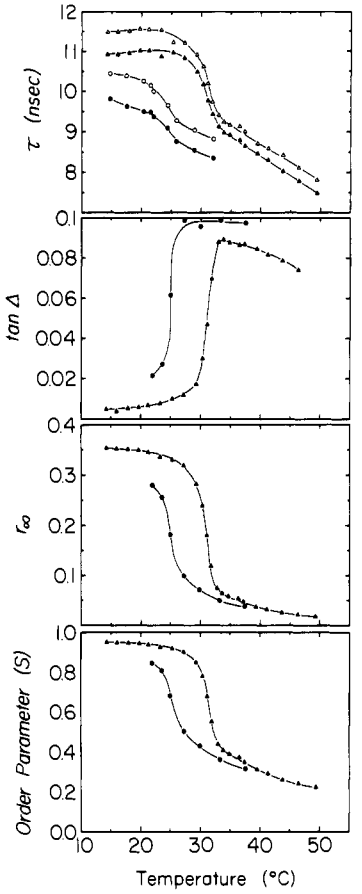

FIGURE 4: Effects of melittin on temperature transition profiles on DMPC using DPH as a fluorescent probe. Circles show data for DMPC and triangles data for MLT–DMPC complexes. (Top panel) The phase and modulation lifetimes of DPH in DMPC and MLT–DMPC complexes as temperature is increased: open symbols denote τ_m (modulation); closed symbols denote τ_ϕ (phase). (Second panel) Differential tangent data. (Third panel) r_∞ (limiting hindered anisotropy) data. (Bottom panel) Plots of order parameter.

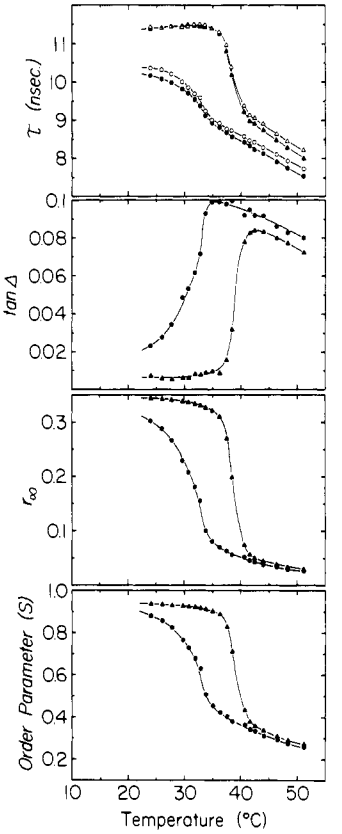

FIGURE 5: Changes in fluorescence lifetimes (τ), differential tangents (tan Δ), limiting hindered anisotropies (r_∞), and order parameters for DPH embedded in DPenPC vesicles and in melittin–DPenPC complexes as temperature is varied. In the uppermost panel (●) and (○) represent lifetimes measured by phase (τ_ϕ) and modulation (τ_m) for DPH in DPenPC vesicles only, while (▲) and (△) give τ_ϕ and τ_m for DPH in MLT–DPenPC complexes. In the three lower panels tan Δ, r_∞, and S data for DPH in DPenPC vesicles and in MLT–DPenPC complexes are given and denoted by (●) and (▲) for the two systems, respectively. T_c for the lipid vesicles was 32 °C and for the mixed micelle was 40 °C.

complexes were also seen at peptide:lipid ratios >1:50. In all micrographs of MLT–lipid complexes, increased rouleaux formation was evident; this was minimal at low MLT:lipid ratio but progressively more marked as the ratio increased. The rouleaux had the appearance of stacked disks, each disk being approximately 40-Å thick. Rouleaux were especially common in micrographs of melittin–DMPC complexes that had been heated to 40 °C and then cooled to room temperature, irrespective of the peptide:lipid ratio.

In Figures 3–5 the effects of temperature on the fluorescence anisotropy of DPH embedded in DMPC and DPenPC vesicles and in DMPC–MLT and DPenPC–MLT complexes are shown. Clearly, melittin alters the thermotropic behavior of both DMPC and DPenPC. The T_c is shifted upward from 24 to 32 °C for DMPC and from 33 to 41 °C for DPenPC, but the cooperative nature of the phase transition is retained and possibly even accentuated. The pattern observed here is typical for melittin complexes with either DMPC or DPenPC at MLT:lipid ratios >1:400 and <1:100. At $T < T_c$ for the melittin–lipid and unilamellar vesicles, the steady-state anisotropies for DPH are higher in the melittin–lipid complexes than in the original lipid preparation. At peptide:lipid ratios ≥1:100, the transition broadens and at very high ratios (1:1) disappears altogether (Figure 3).

The data in Figures 4 and 5 provide an even clearer demonstration of the thermotropic response of the melittin–lipid complexes reflected in the fluorescence properties of DPH.

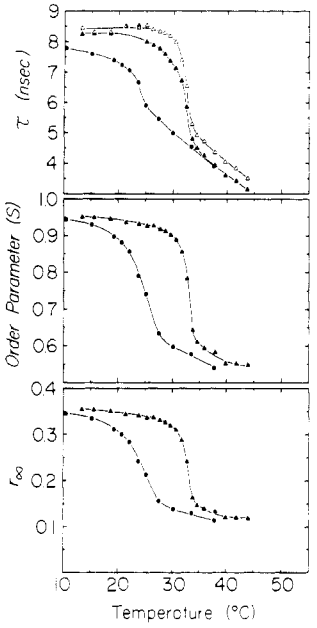

FIGURE 6: Changes in fluorescence lifetimes (τ), r_∞, and order parameter (S) for TMA-DPH in DMPC vesicles and MLT–DMPC complexes. Fluorescence lifetimes by phase (τ_ϕ) and modulation (τ_m) for TMA-DPH in DMPC vesicles [τ_ϕ (●)] and MLT–DMPC [τ_ϕ (▲); τ_m (△)] are given in the upper panel. r_∞ and S values for TMA-DPH in DMPC (●) and MLT–DMPC complexes (▲) are given in the middle and lower panels.

The fluorescence lifetimes (τ) of the probe were noticeably higher and more homogeneous (i.e., τ determined by phase, [τ_ϕ], and τ determined from modulation measurements, [τ_m], were the same within experimental error) at $T < T_c$ for the complexes as compared to the vesicles (see legends to Figures 4 and 5). The r_∞ values and their transform (i.e., order parameters) indicate that DPH is indeed more highly ordered in the peptide–lipid complexes than in the vesicles at $T < T_c$ but that the lipid does possess a highly cooperative order–disorder transition as had been shown by the steady-state anisotropy data.

Although it was a remote possibility, not suggested by the data, DPH might have partitioned in the vicinity of the peptide per se in the MLT–lipid complex. If that were so, then the changes in its fluorescence could have been reflecting a unique population of lipid molecules. However, a cationic derivative of DPH, TMA-DPH, should be electrostatically repelled from the environs of the melittin and should therefore probe the lipid only. The fluorescence depolarization data for TMA-DPH are shown in Figure 6; qualitatively, they are the same as those for DPH although quantitatively the values were, as expected, quite different (Prendergast et al., 1981).

There is a distinct possibility that the anisotropy signals observed at T_c for the melittin–lipid complex could reflect the dissociation of melittin from the lipid with subsequent cooperative change in phase of the "freed" lipid domain. If this were so, then we might anticipate that there would be significant differences in the thermotropic response of the lipid when measurements were made as the sample was heated to $T > T_c$ or, alternatively, cooled from temperatures greater than T_c. However, in Figure 7 we show that there was little difference between the heating and cooling curves for either the melittin–DMPC or the melittin–DPenPC complex as monitored by changes in DPH fluorescence anisotropy. Further information on the thermotropic transitions was obtained from QLS (Figure 8). The size of complexes increases markedly as the temperature is increased through T_c and attains a

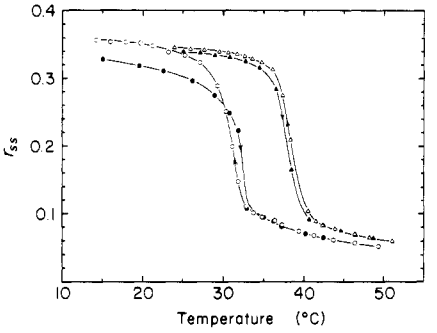

FIGURE 7: Variation in steady-state anisotropies for DPH embedded either in MLT–DMPC (circles) or in MLT–DPenPC (triangles) complexes as temperature is first increased beyond T_c and then to $T < T_c$ of the system under study. The MLT:lipid ratio was 1:100. Samples were held at each temperature (±0.10 °C) for at least 30 min to ensure equilibrium conditions. The arrows indicate the direction of the temperature change.

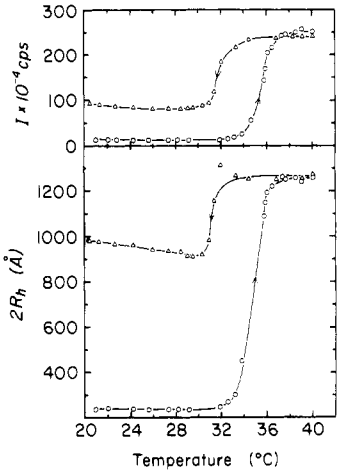

FIGURE 8: Variation in light scattering intensities (upper panel—y axis) and diameters (lower panel) of melittin–DMPC complexes as MLT–lipid mixed micelles (at 1:100 molar ratio of peptide:lipid) are heated and cooled. In both the upper and lower panels the circles and triangles represent data taken while the temperature was scanned up and down, respectively. The data were corrected for viscosity changes induced in the solvent by the change in temperature. These data were obtained by quasi-elastic laser light scattering.

plateau value at $T > T_c$. We estimate the ratio of maximum and minimum molecular weights to be 12.5 on the basis of the total scattering intensities. The apparent thermal transition temperature determined from these data is 35 °C, 3 °C higher than estimated from DPH anisotropy data. When the complexes are cooled from 42 to 20 °C, their apparent size decreases but only to a final diameter of ~*950* Å, *not* to the original 220 Å. Hysteresis is evident.

Discussion

The data that we have presented illustrate the complexity of the interaction of melittin with the saturated glycerophosphocholines, DMPC and DPenPC. Our results differ significantly from all other reports in the literature on protein–lipid complexes and indicate that there are several features unique to the melittin–lipid interaction. In this discussion we try to rationalize our data in terms of structures formed and mechanism of interaction but at the outset acknowledge that a full interpretation is not yet possible.

Melittin obviously can interact with lipid vesicles at temperatures above or below the phase transition temperature. The data we present indicate, however, that the maximal rate at which vesicles of DMPC and DPenPC are disrupted by

melittin is found at the phase transition temperatures of each lipid. The multistep nature of the interaction is best shown by the light scattering data. We infer that the initial increase in light scattering is due to aggregation of vesicles (Figure 1) and that the subsequent marked decrease signals formation of a stable mixed micelle at equilibrium. At the present time we do not know at what stage lysis of the vesicles occur. But it is clear that the final particle is nonvesicular and relatively homogeneous in size; the actual dimensions of the mixed micelle vary with peptide:lipid ratio. This conclusion is supported by several data. (i) On the basis of total light scattering intensity changes, the molecular weight ratio of the vesicles and mixed micelles is ca. 11. This agrees roughly with the calibrated reduction in molecular weight estimated from the radii of the vesicles and mixed micelles, when the polydispersity of the sample is taken into account (Selser & Yeh, 1976; J. Wei, unpublished calculations). Furthermore, the decrease in the quality factor when the MLT–lipid micelle is formed (Table I) indicates that these species have a more homogeneous size distribution than the original vesicles. The light scattering data are corroborated by the results of electron micrography. (ii) All of the contents of the vesicles are released during the interaction of melittin. Gel filtration experiments [done by HPLC and also by standard chromatographic methods on agarose A-15 columns—F. G. Prendergast (unpublished data)] showed that no [^{14}C]inulin was retained in the lipid fraction subsequent to interaction with [^{14}C]inulin-loaded DMPC vesicles. (iii) While the electron micrographs cannot *prove* the existence of *nonvesicular particles*, they do show "stacked disks" (rouleaux) in the melittin–lipid complexes akin to those observed in apolipoprotein–DMPC mixed micelles (Wlodawer et al., 1979); the latter have been assumed to be flattened, discoid structures. This latter point is especially important in view of the thermotropic changes described below.

The multiphasic change in lipid architecture evinced by the quasi-elastic light scattering data is also reflected in the time-dependent change of fluorescence anisotropy of DPH embedded in the lipid. The latter shows a biphasic increase in anisotropy. The two phases correspond to the increase and decrease in the light scattering signal, respectively, although the anisotropy changes suggest only a progressive *increase* in lipid order as the peptide–lipid interaction proceeds. These anisotropy data imply that if the first phase is indeed due to aggregation of the vesicles, aggregation occurs with an increase in lipid order. What this may mean with respect to mechanism of lipid fusion is not at all clear from our data. Although we know from changes in the intrinsic fluorescence of the melittin that the peptide does bind to DMPC and DPenPC vesicles, both below and above their T_c values, there is little change in light scattering signal or in the anisotropy of DPH under such conditions of interaction. This implies that the perturbation of the lipid milieu is minimal at $T \ll T_c$ or $T \gg T_c$.

The thermotropic behavior of the mixed (MLT–lipid) micelle is obviously completely different from that of the parent lipid. The steady-state anisotropy and differential phase fluorometric data in Figures 3–6 show that the phase transition temperatures of the lipids have been shifted up ~8 °C in the mixed micelle compared to that in the parent lipid. The high order of the system at $T < T_c$ is clearly reflected in the high values for r_{ss} and the order parameters shown in Figures 4 and 5 and the homogeneous lifetimes ($\tau \simeq \tau_m$) for the probe. The phase change in the lipid domain remains obviously cooperative, despite the reduction in size (i.e., increased radius of curvature relative to the original vesicles). Such cooperativity implies that the basic bilayer structure of the lipid is maintained in the mixed micelle and that the cooperative unit has not been significantly reduced (compare the profiles of the changes in r_{ss} or S for the micelles with those for the original vesicles).

The sharp phase transition profile may also imply that MLT is distributed uniformly or in a statistically random fashion among the fixed micelles. That is, there is not a population of micelles with particularly high local concentration of melittin. The phase transition profile begins to broaden perceptibly only when the peptide:lipid ratio is in excess of 1:75. The anisotropy profile observed for a 1:1 peptide–lipid mixture indicates a completely disordered mixed micelle.

Although it seems unlikely, DPH might have partitioned into unique peripeptide domains of lipid. (Note, although melittin itself forms tetrameric "micelles", DPH does not significantly partition into such species.) The fluorescence signals emitted from such domains might then reflect the behavior of a unique lipid population rather than the bulk lipid. To obviate this interpretation, we performed experiments with TMA-DPH. This cationic analogue of DPH (Prendergast et al., 1981) would be expected to partition away from the hexacationic melittin molecule and therefore would reflect the behavior of the "bulk" lipid fraction of the mixed micelle. The results in Figure 6 show the qualitative similarity of the DPH and TMA-DPH behavior, from which we infer that DPH is not uniquely distributed in a unique lipid domain.

The thermotropic behavior of the mixed micelle is unusual in other ways. For example, the r_{ss} data support a complete reversibility in apparent lipid order of the mixed micelle as temperature is changed up and down through T_c; these measurements were made with the system at equilibrium at each temperature. The QLS data, however, show a hysteretic response. There is a sharp increase in apparent micellar size at T_c. The ratio of sizes above and below T_c (as temperature is scanned from below) is 5.2. QLS shows that the mixed micelles do not return to their initial size upon cooling although the DPH anisotropy changes indicate a return to the state of order of the originally formed peptide–lipid micelle. Electron microscopy indicates that a heating–cooling cycle leads to appearance of a large number of stacked disks—rouleaux—when the recooled mixture is examined. However, the average diameter of each of the "disks" in the rouleaux was ~230 Å, i.e., approximately the same as the "original" mixed micelle. The preponderance of these rouleaux in the recooled mixed micelles explains the apparent increase in molecular dimensions and the total scattering intensity determined by QLS.

We do not know the structural basis of the changes in either light scattering or DPH anisotropy at T_c for the mixed micelles. One possibility is that the large increase in light scattering at T_c is due to revesiculation. However, two facts argue against such a conclusion. First, by following changes of intrinsic tryptophan fluorescence of melittin complexed with lipid, we have shown that the peptide remains associated with the lipid through the phase transition in either a heating or cooling cycle (F. G. Prendergast, unpublished results). Second, the reversibility of the DPH anisotropy changes observed in Figure 5 show that the fundamental organization of the mixed micelle must not be changing throughout the phase transition. We may rationalize the latter conclusion in the following manner. We have already shown that melittin–lipid mixed micelles effectively form only at the thermal transition temperature of the lipid (i.e., 24 °C for DMPC). Let us suppose that at the thermal transition of the mixed micelle the lipid re-formed vesicles. We would then anticipate effective reinteraction of melittin to occur at 24 °C in a cooling cycle. The

anisotropy data show, however, that the heating and cooling curves are essentially superimposable. Clearly, we do not yet have a satisfactory explanation of the behavior of the mixed micelles in their phase transition region.

Our results indicate that while the interaction of melittin with DMPC and DPenPC has some features in common with the lipid binding of other amphipathic helices such as apolipoproteins, there are substantial differences. These appear both in the kinetics of the interaction and in the nature of the final complex. Many proteins and peptides are known to interact optimally at the T_c of lipids; the most apposite examples for our purposes are probably the interactions of apolipoproteins with DMPC (Morrisett et al., 1977; Gilman et al., 1981; Jonas & Drengler, 1980; Jonas & Mason, 1981; Pownall et al., 1978). Also, apolipoprotein A_1 (apo-A_1) is known to form discoid structures when reacted with DMPC at 24 °C (Wlodawer et al., 1979; Jonas & Drengler, 1980). But here the similarities end. For example, Jonas & Drengler (1980) showed (on the basis of time-dependent changes in DPH fluorescence anisotropy that attended interaction of apo-A_1 with DMPC at 25 °C) that the apo-A_1–lipid interaction was first order. In contrast, the MLT–DMPC interaction is clearly not first order when we consider either the light scattering or DPH anisotropy data. Further, although apolipoprotein A_1–DMPC mixed micelles also exhibit an elevated T_c, the elevation is only 3–4 °C, and the transition is broadened (Jonas & Mason, 1981). This is to be compared with an 8 °C shift in T_c and a "sharp" phase transition profile observed in the MLT complexes with DMPC and DPenPC. Our data are also at odds with those of others who have studied interaction of MLT with lipids. Mollay (1976) used differential scanning calorimetry and Lavialle et al. (1980) and Levin et al. (1982) used Raman spectroscopic techniques to show that melittin–DMPC mixed micelles at peptide:lipid ratios of 1:25 and 1:14 exhibited biphasic phase transitions. One transition occurred at 19 °C and the other at 29 °C, and both were distinctly broad. They ascribed the transition at 29 °C to melting of boundary lipid and calculated that the number of lipid molecules in this boundary layer varied with the peptide:lipid ratio. Our data do not show such transitions and obviously do not support the existence of such boundary lipid. But it is possible to explain the disparities between our data and those of Mollay & Kreil (1973) and Levin et al. (1982). Two aspects of their experiments stand out. First, they used relatively high lipid:peptide ratios. From our data at similar ratios, DPH anisotropy changes do not reveal biphasic thermotropic transitions. Second, they reacted the peptide and lipid at 40 °C for 1 h and assumed that the interaction was complete; subsequent measurements were made on samples first cooled to ca. 10 °C. Since melittin interacts optimally at T_c, it seems likely that their studies were performed on a melittin–DMPC system that had not at any time attained equilibrium although some complex must have formed as the melittin–DMPC mixture was cooled through the thermal transition of the DMPC en route to 10 °C.

We may therefore conclude that melittin interacts optimally with DMPC at the phase transition temperature of the lipid to form, at equilibrium, a stable mixed micelle. Such interaction is not apparently dependent on chain length since similar results are obtained in the melittin–DPenPC and melittin–DEPC systems. This mixed micelle is most likely a disklike particle with highly ordered lipid arranged in a bilayer. This latter conclusion is not uniquely ours; Podo et al. (1982) have also reported that melittin does not disrupt the bilayer organization of egg lecithin vesicles although it clearly lyses such vesicles. The mechanism whereby the peptide organizes the lipid is not at all clear, and the effects of melittin in this regard are, as far as we know, unique among peptides interacting with lipids. Fatty acids when mixed with saturated phosphatidylcholines are also capable of raising the phase transition temperature of the lipid. However, it is improbable that a mechanism akin to this operates in the melittin–lipid mixed micelle, for two reasons. First, fatty acids have to be used in high molar ratios to cause such effects (Mabrey & Sturtevant, 1977); melittin is obviously effective at molar ratios as low as 1:400 and possibly lower. Second, fatty acids are probably effective because they can intercalate between the fatty acyl moieties of the lipid and thereby enhance packing of fatty acyl chains. It is improbable that amino acid side chains, even of leucine and isoleucine moieties, could promote such interactions in the lipid milieu. Rather, we would expect that the inevitably irregular surface of the peptide would exert a disordering rather than an ordering effect on the lipid. Disordering effects of melittin *are* noted but only at peptide:lipid ratios in excess of 1:75 (Figure 3).

Until we know more about the disposition of the peptide in the complex, and the specific roles of the hydrophobic regions and the hexacationic hexapeptide at the carboxyl terminus in the interaction, we can in no way explain the thermotropic behavior of the melittin–lipid mixed micelle. Circular dichroism data (Dawson et al., 1978) and infrared spectroscopic (Lavialle et al., 1982) data show that lipid-bound melittin is helical. The elegant NMR data of Wüthrich and co-workers (Lauterwein et al., 1979, 1980; Brown et al., 1980, 1982) have revealed that the melittin molecule is rigidly held in melittin–lipid complexes. Further, by comparison of the NMR spectra of tetrameric and lipid-bound MLT, the authors did not find evidence that the peptide was aggregated in the lipid. In contrast, Georghiou et al. (1981), on the basis of the similarity between fluorescence spectra and lifetimes of tetrameric melittin in aqueous solution and lipid-bound MLT, have suggested that the peptide is tetrameric when bound to lipids. But while all of these studies yield information on the lipid-bound conformation of the peptide, they cannot provide any insight into the structure of the melittin–lipid mixed micelle per se, *especially* at the low melittin:lipid ratios we have employed.

Further studies to characterize the structure of the mixed micelle are clearly indicated. It would be especially interesting to know, for example, whether melittin forms "bicycle tire" mixed micelles (Segrest, 1979; Wlodawer et al., 1979), i.e., discoid structures with melittin on the periphery. It is important to determine whether melittin interacts in a similar fashion with negatively charged phospholipids. Further, we must ascertain whether other amphipathic peptides, most notably δ-hemolysin (Fitton et al., 1980), or synthetic amphipathic peptides (Fukushima et al., 1979; DeGrado et al., 1981, 1982) behave similarly to melittin.

Finally, we need to make a few general observations. The lytic effects of melittin obviously do not require the formation of these unique mixed micelles since the peptide interacts with and lyses lipid vesicles at temperatures well above the thermal transition temperature. Our data sound a cautionary note: it is obviously advisable to use more than one physical technique to determine whether one has an equilibrium system prior to pursuing studies of the thermotropic behavior of peptide–lipid or protein–lipid complexes. And lastly, it is very likely that the physical chemistry of mixed peptide–lipid micelles will often be dependent on the thermal history of the sample, much as the melittin–lipid complex demonstrates.

Boggs et al. (1981) have made a similar point for myelin–basic protein–lipid mixtures.

Acknowledgments

We thank E. Webster for typing the manuscript, P. Callahan for preparing the figures, and Greg Hadley for his assistance with the electron microscopy of the lipid vesicles and melittin–lipid complexes.

References

Bloomfield, V. A., & Lim, T. K. (1978) *Methods Enzymol. 48*, 415.

Boggs, J. M., Stamp, D., & Moscarello, M. A. (1981) *Biochemistry 20*, 6066.

Brown, L. R., Lauterwein, J., & Wüthrich, K. (1980) *Biochim. Biophys. Acta 622*, 231.

Brown, L. R., Braun, W., Kumar, A., & Wüthrich, K. (1982) *Biophys. J. 37*, 319.

Dawson, C. R., Drake, A. F., Helliwell, J., & Hider, R. C. (1978) *Biochim. Biophys. Acta 510*, 75.

DeBony, J., DuFourcq, J., & Clin, B. (1979) *Biochim. Biophys. Acta 552*, 531.

DeGrado, W. F., Kezdy, F. J., & Kaiser, E. T. (1981) *J. Am. Chem. Soc. 103*, 679.

DeGrado, W. F., Musso, G. F., Lieber, M., Kaiser, E. T., & Kezdy, F. J. (1982) *Biophys. J. 37*, 329.

Dufourcq, J., & Faucon, J.-F. (1977) *Biochim. Biophys. Acta 467*, 1.

Ellefson, R. D., & Caraway, W. T. (1976) in *Fundamentals of Clinical Chemistry* (Tietz, N. W., Ed.) pp 474–541, Saunders, Philadelphia, PA.

Engel, L. W., & Prendergast, F. G. (1981) *Biochemistry 20*, 7338.

Fitton, J., Dell, A., & Shaw, W. V. (1980) *FEBS Lett. 115*, 209.

Fukushima, O., Kupferberg, J. P., Yokoyama, S., Kroon, D. J., Kaiser, E. T., & Kezdy, F. J. (1979) *J. Am. Chem. Soc. 101*, 3703.

Georghiou, S., Thompson, M., & Mukhopadhyay, A. K. (1981) *Biochim. Biophys. Acta 642*, 429.

Gilman, T., Kauffman, J. W., & Pownall, H. J. (1981) *Biochemistry 20*, 656.

Habermann, E. (1965) *Science (Washington, D.C.) 177*, 314.

Hegner, D., Schummer, U., & Schnepel, G. H. (1973) *Biochim. Biophys. Acta 291*, 15.

Hendrickson, H. S., & Rauk, P. N. (1981) *Anal. Biochem. 116*, 553.

Heyn, M. (1979) *FEBS Lett. 108*, 359.

Jähnig, F. (1979a) *Proc. Natl. Acad. Sci. U.S.A. 76*, 6361.

Jähnig, F. (1979b) *J. Chem. Phys. 70*, 3279.

Jonas, A., & Drengler, S. M. (1980) *J. Biol. Chem. 255*, 2190.

Jonas, A., & Mason, W. R. (1981) *Biochemistry 20*, 3801.

Kanellis, P., Romans, A. Y., Johnson, B. J., Kercret, H., Chiovetti, R., Jr., Allen, T. M., & Segrest, J. (1980) *J. Biol. Chem. 255*, 11464.

Knöppel, E., Eisenberg, D., & Wickner, W. (1979) *Biochemistry 18*, 4177.

Koppel, D. E. (1972) *J. Chem. Phys. 57*, 4814.

Lakowicz, J. R., & Prendergast, F. G. (1978) *Biophys. J. 24*, 213.

Lakowicz, J. R., & Prendergast, F. G., & Hogen, D. (1979) *Biochemistry 18*, 508.

Lauterwein, J., Bösch, C., Brown, L. R., & Wüthrich, K. (1979) *Biochim. Biophys. Acta 556*, 244.

Lauterwein, J., Brown, L. R., & Wüthrich, K. (1980) *Biochim. Biophys. Acta 622*, 219.

Lavialle, F., Levin, I. W., & Mollay, C. (1980) *Biochim. Biophys. Acta 600*, 62.

Lavialle, F., Adams, R. G., & Levin, I. W. (1982) *Biochemistry 21*, 2305.

Levin, I. W., Lavialle, F., & Mollay, C. (1982) *Biophys. J. 37*, 339.

Lipari, G., & Szabo, A. (1980) *Biophys. J. 30*, 489.

Mabrey, S., & Sturtevant, J. M. (1977) *Biochim. Biophys. Acta 486*, 444.

Mantulin, W. W., & Weber, G. (1977) *J. Chem. Phys. 66*, 4092.

Mao, S. J. T., Jackson, R. L., Gotto, A. M., Jr., & Sparrow, J. T. (1981) *Biochemistry 20*, 1676.

Mollay, C. (1976) *FEBS Lett. 64*, 65.

Mollay, C., & Kreil, G. (1973) *Biochim. Biophys. Acta 316*, 196.

Morrisett, J. D., Jackson, P. L., & Gotto, A. M. R. (1977) *Biochim. Biophys. Acta 472*, 93.

Pletcher, C. H., Resnick, R. M., Wei, G. J., Bloomfield, V. A., & Nelsestuen, G. L. (1980) *J. Biol. Chem. 255*, 7433.

Podo, F., Strom, R., Crifo, C., Berthet, C., Zulauf, M., & Zaccai, G. (1982) *Biophys. J. 37*, 161.

Pownall, H. J., Massey, J. B., Kusserow, S. K., & Gotto, A. M., Jr. (1978) *Biochemistry 17*, 1183.

Prendergast, F. G. (1981) *Period. Biol. 83*, 69.

Prendergast, F. G., Haugland, R. P., & Callahan, P. J. C. (1981) *Biochemistry 20*, 7333.

Segrest, J. P. (1979) *FEBS Lett. 106*, 169.

Selser, J. C., & Yeh, Y. (1976) *Biophys. J. 16*, 847.

Sessa, G., Freer, J., Colacicco, G., & Weissmann, G. (1969) *J. Biol. Chem. 244*, 3575.

Spencer, R. D., & Weber, G. (1969) *Ann. N.Y. Acad. Sci. 158*, 361.

Spencer, R. D., & Weber, G. (1970) *J. Chem. Phys. 52*, 1654.

Tosteson, M. T., & Tosteson, D. C. (1981) *Biophys. J. 36*, 109.

Weber, G., & Bablouzian, B. (1966) *J. Biol. Chem. 241*, 2558.

Williams, J., & Bell, R. (1972) *Biochim. Biophys. Acta 288*, 255.

Wlodawer, A., Segrest, J. P., Chung, B. H., Chiovetti, R., Jr., & Weinstein, J. N. (1979) *FEBS Lett. 104*, 231.

Yunes, R., Goldhammer, A. R., Garner, W. K., & Cordes, E. H. (1977) *Arch. Biochem. Biophys. 183*, 105.